International Journal of Engineering & Technology, 7 (2.7) (2018) 642-646

International Journal of Engineering & Technology

Website: www.sciencepubco.com/index.php/IJET

Research Paper

Improvement of position and orientation of Unmanned Arial Vehicle (UAV) with INS/ GPS

V.Appala Raju[1], P.Vasundhara[2],V.ChandraKanth Reddy[2], A.Sai Aiswarya[2]

Research Scholar[1], Student[2] ,Department of ECE, Koneru Lakshmaiah Education Foundation, Vaddeswaram, Guntur, Andhra Pradesh, India – 522502.
**Email: appalarajuvadaboyina@gmail.com*

Abstract

This paper deals with the methods performing state estimation .that is position and orientation of Unmanned Arial Vehicle (UAV) using GPS, gyro, accelerometers and magnetometer sensors. Various methods are designed for position and orientation measurements of UAV. In this paper we proposed extended kalman filter based inertial navigation system using quaternions and 3D magnetometer. Initially we load UAV truth data from a file ,generate noisy UAV sensor measurements and perform UAV state estimation and display UAV state estimate results with proposed method compares with previously exited method extended kalman filter based altitude and heading reference system using quaternion and 3D magnetometer simulation .Results shows that EKF-INS method gives better position and orientation of UAV.

Keywords: *UAV, INS, GPS, Extended Kalman Filter, Attitude and heading reference system.*

1. Introduction

In present days UAV's have been progressively utilized for extensive variety of uses, those are aviation, agribusiness, development, looking over et cetera. How these UAV's working securely by create dependable route and control innovations for UAV's position.

Now a days, the generally utilized route advancements for UAV's are GPS beneficiaries and INS gadgets and a video framework. INS gadgets don't rely upon the outside radio estimations. It monitors its situation by precisely estimating accelerometers and spinner readings. That is the reason it works in remote territories without ground based navigational guides. At the point when contrasted with INS here and now situating precision, GPS route advancements give predictable exactness, when it tracks adequate GPS signals amid the whole UAV mission; however drawback in GPS is it doesn't give elevation estimation. That is the reason coordinated GPS/INS route framework utilized for some applications; however execution of the incorporated framework predominantly relies upon the accessibility and nature of GPS signals [1-3, 7].

2. Vision Aided Movement Estimation

Enormous scopes of creative and perceptive sensors are to be needed to meet the prerequisite of this remarkable programming, which gives an adaptable improvement to the coordinated device. The investigation of visual movement assessment comprises basic issues. One of them is to decide optical drift and additionally trademark corresponding from photograph successions, and the inverse is to evaluate development parameters and utilization of them. Some scientists made an evaluation at calculations for estimation of movement/shape parameters from picture groupings inside the PC vision setting. Keeping in mind the end goal to ideally join vision component into a GPS/INS route device, the creative and insightful route execution should be examined first.

The photograph successions taken from the UAV can be utilized as a different arrangement of independent spatial estimations. Given that close contraptions flaunt a superior precise development inside the visual field than far off items, optic buoy can be utilized to ascertain the assortment to work area bound protests inside the field of view, or the bona fide pace of devices with perceived levels. In this mission, optic take the path of least resistance is ascertained on the UAV helicopter progressively at 50Hz the utilization of a photo interjection set of guidelines (Srinivasan, 1994), which is capable in common out of entryways conditions and in the state of precise rates of unmistakable development.

Two stages are required to decide interpretation speeds from the optic float determined precise expenses. Right off the bat, the impacts of turn are isolated from the ones interpretations through subtracting the recognized revolution cites, estimated with the guide of the locally available charge whirligigs, from the optic take the path of least resistance cites. Furthermore, the picture movement expense is enhanced by utilizing the range over the floor anticipated that through a LRF would evaluate the mean-centred measurement of parallel and longitudinal speeds. The vertical speed in respect to the floor can be computed by means of the span of LRF. As the majority of the sensors have measurement botches, the critical thing issue appropriate here is to model and gauge the errors and concentrate the route data from the inventive and perceptive and INS information streams[8-13].

Therefore, the frame which contains UAV horizontal speed can be calculated with the help of optical drift.

With the use of following formula LRF and gyro can be modified angularly.

$$v_{bxy} = (\delta_{xy} - \varphi_{xy}) * r_{gz} \quad (1)$$

Copyright © 2018 Authors. This is an open access article distributed under the Creative Commons Attribution License, which permits unrestricted use, distribution, and reproduction in any medium, provided the original work is properly cited.

Wherein v_{bx} is the horizontal translation velocity; δ_{xy} is the size of angular price's optical waft; φ_{xy} is the rotation charges of horizontal axis; r_{gz} is relative peak from the floor of LRF. The integration glide chart is proven in Fig.1

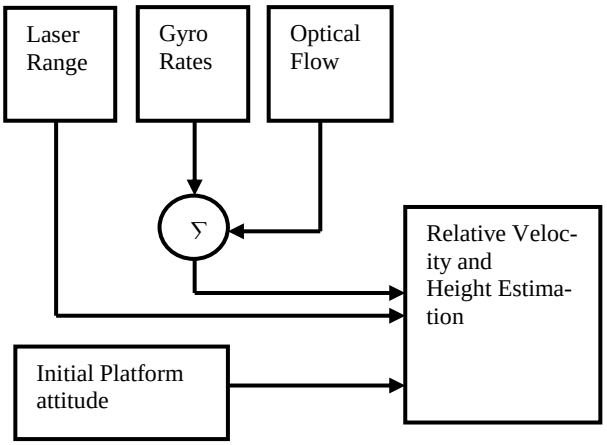


Fig.1: Flow chart for Vision based navigation system.

This proposed model is not effective and contains many errors which may contain small constant offset (likely 10cm) and a small scale blunders (<1%) from LRF. Other errors which can be found are scale errors from optic glide. Additional errors which can be seen are the errors from gyros. Other mistakes consist of error in attitude and the slope of the floor etc. The most important errors can be reduced by following GPS technique.

3. GPS/VISION/GYRO Navigation

The following is the flow chart of GPS/INS/Vision navigation integrated device which mainly uses two Kalman filters.

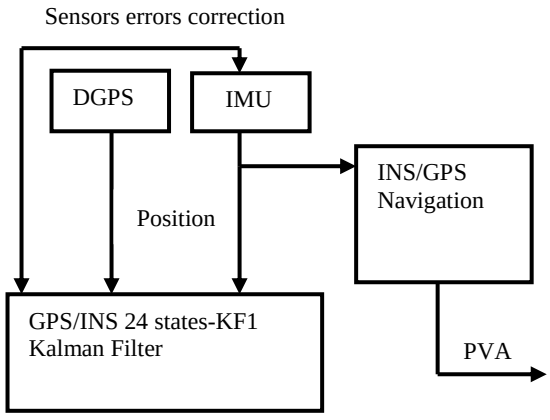


Fig.2: DGPS/INS/vision integrated system flowchart

When errors are seen in GPS, to update or modify the errors in the KF1 and to know the mistakes in INS and to modify the navigation errors which results in change in the GPS, positioning results are used. Simultaneously mistakes in LRF and optic drift can be identified by the GPS derived velocity in Kalman Filter (KF2). Asa result of these correct measurements from gyro, optic flow and LRF can be obtained which gives the exact values of horizontal velocity and height above the floor [4,6,7]

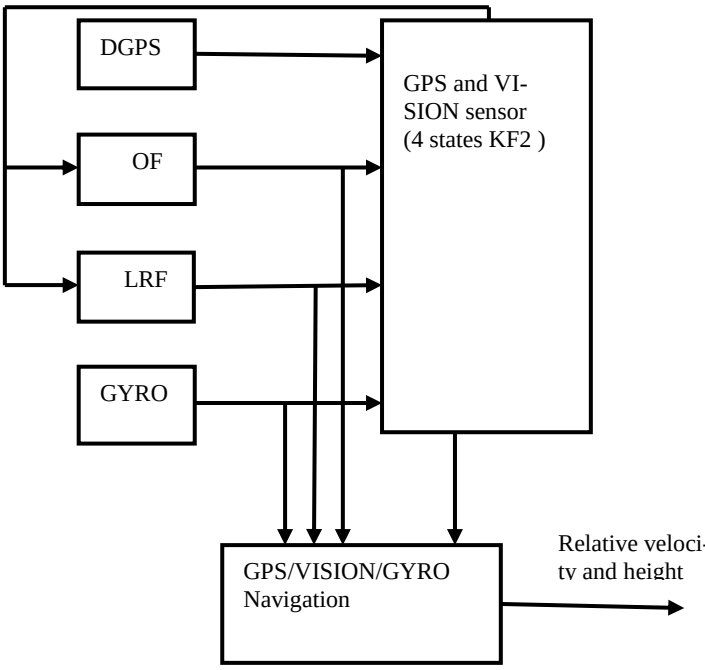


Fig.3: GPS/INS/vision integrated system flowchart

$$x_k = \varphi_{k-1} x_{k-1} + w_{k-1} \quad (2)$$

$$z_k = H_k x_k + v_k \quad (3)$$

Wherein x_k is state vector of order (n*1), φ_k is transition matrix of order (n×n), z_k is (r×1) observation vector, H_k is observation matrix of order (r×n). w_k and v_k are uncorrelated white Gaussian noise.

The KF2 error states are:

$$x_{GI} = [X_{Nav} X_{Acc} X_{Gyro} X_{Grav} X_{Ant}]^T \quad (4)$$

Where in

$$\begin{aligned} X_{Nav} &= [\delta\gamma_N, \delta\gamma_E, \delta\gamma_D, \delta r_N, \delta r_E, \delta r_D, \delta v_N, \delta v_E, \delta v_D]a \\ X_{Acc} &= [\nabla_{ax}, \nabla_{ay}, \nabla_{az}, \nabla_{bx}, \nabla_{by}, \nabla_{bz}] \\ X_{Gyro} &= [\phi_{bx}, \phi_{by}, \phi_{bz}] \\ X_{Grav} &= [\delta g_N, \delta g_E, \delta g_D] \\ X_{Ant} &= [\delta l_x, \delta l_y, \delta l_z] \end{aligned} \quad (5)$$

The following entire terrestrial INS psi-angle errors can be seen within the system:

$$\begin{aligned} \bullet \quad \delta v &= -(\beta_{ie} + \beta_{in}) * \delta r - \delta v * f + \delta g + \phi \\ \bullet \quad \delta r &= -\beta_{en} * \delta\gamma + \delta r \\ \bullet \quad \delta\gamma &= -\beta_{in} * \delta v + \varepsilon \end{aligned} \quad (6)$$

The observation vector z consists of $\delta r_N, \delta r_E, \delta r_D$

$$z(t) = [P_{INS} - P_{GPS}]^T = [I_{3*3} O_{3*2}] x_{GI} + v(t) \quad (7)$$

Wherein P_{INS} is INS measured position and P_{GPS} is GPS measured position.

3.1. Modelling Error Estimation for Vision Sensors

The entire document should be in Times New Roman. The font sizes to be used are specified in Table 1. As seen in Section 3.1, there are various errors sources in the Equation (1).Fixed offset and a scale mistakes are incorporated from the height of LRF. Scale errors in optic flow are seen as two instructions. Therefore 4 states are used to interpret the errors Kalman filter.

$$x_{LOF} = [\delta\alpha_b, \delta\alpha_f, \delta\omega_{fx}, \delta\omega_{fy}] \quad (8)$$

Wherein $\delta\alpha_b$ is LRF constant offset, $\delta\alpha_f$ is size error, $\delta\omega_{fx}$ is optic float scale errors at x axis, $\delta\omega_{fy}$ is optic float scale errors at y axis.

The zero-mean Gaussian white noise which is dynamic version of these 4 error states is treated as follows:

$$x_{LOF} = \omega_{LOF} \quad (9)$$

$$z_{LOF}(t) = [H^V{}_{LOF} - H^V{}_{GPS}]^T = [Q_{2*4}]x_{LOF}(t) + r_{2*1}(t) \quad (10)$$

Wherein $H^V{}_{LOF}$ is horizontal velocity of LOF and $H^V{}_{GPS}$ is horizontal velocity of GPS.

As per Equation (1) and Equation (8) the LRF navigation errors and optical flow is derived as:

$$v_{gxy} = [\beta_{xy} * (1 - \omega_{fxy}) - \varphi_{xy}] * (r_{gz} - \alpha_b) * (1 - \alpha_f) + \varepsilon \quad (11)$$

Wherein ε is bias from the ground surface and other errors. The error model for Kalman Filter can be given as:

$$\delta_{gxy} = (r_{gz} - \alpha_b) * (1 - \alpha_f)\delta\omega_{fxy} + [\beta_{xy} * (1 - \omega_{fxy}) - \varphi_{xy}]$$
$$[(1 - \alpha_f)\delta\alpha_b + (r_{gz} - \alpha_b)\delta\alpha_f] \quad (12)$$

Therefore the H2x4 in Equation (10) is

$$Q_{2*4} = \begin{pmatrix} [\beta_x * (1 - \omega_{fx}) - \varphi_x](1 - \alpha_f) & [\beta_y * (1 - \omega_{fy}) - \varphi_y](1 - \alpha_f) \\ [\beta_x * (1 - \omega_{fx}) - \varphi_x](r_{gz} - \alpha_b) & [\beta_y * (1 - \omega_{fy}) - \varphi_y](r_{gz} - \alpha_b) \\ (r_{gz} - \alpha_b) * (1 - \alpha_f) & 0 \\ 0 & (r_{gz} - \alpha_b) * (1 - \alpha_f) \end{pmatrix}^T \quad (13)$$

4. Methodology

The YAMAHA RMAX Company has been evolved in the period of 1990 by Japan Company. Later, on it led to the invention of the unmanned predator drone in the year 2002 for targeted killing by CIA. Drones has been used for several applications like security ,agriculture .navigation, search and rescue operations etc. but it has been primarily developed for the purpose of agriculture.

4.1 Sensors

Helicopter consists of several sensors inboard in it that is Differential navigation GPS, INS, magnetometer, Laser scanning system, and Charged Coupled Device, camera (imaging payload)[5]. Here the navigation system is a computer program provides information about the graphical images, coordinates and directions on the screen. Camera will be having the basic information including the period of the system configuration. Now–a–days CCD has become one of the major technologies in digital imaging. A charge-coupled device (CCD) is a device for the movement of electric charge, usually from within the device to an area where the charge can be manipulated. LRF is a rotating mirror combined with the RMAX helicopter.

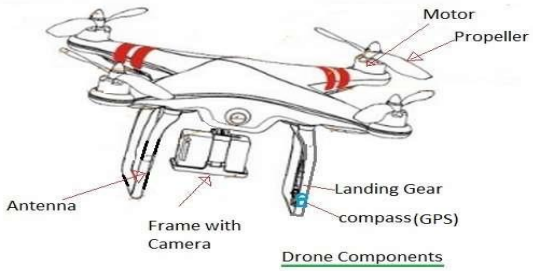


Fig.4: Drone components

4.2 Methods Adopted

4.2.1. Euler angle

4.2.2. Spatial Rotation Using Quaternion

4.2.3. Quaternion

4.2.1 Euler Angle

Euler angle means three angles and is used to describe the rotation of the stiff body with respect to the stationary body. Euler angles are denoted by letters α, β, γ .here the angle α is the circling about the Z axis. The angle β is rounding
About N axis and the angle γ is wheeled about the Z axis. The angle α is amid from *x* axis and the *N* axis. The angle β is in the middle of the *z* axis and the *Z* axis. The angle γ is mid of the *N* axis and the *X* axis .The angle α, γ ranges from 0 to 2π radians , whereas the angle β ranges from 0 to π radians.

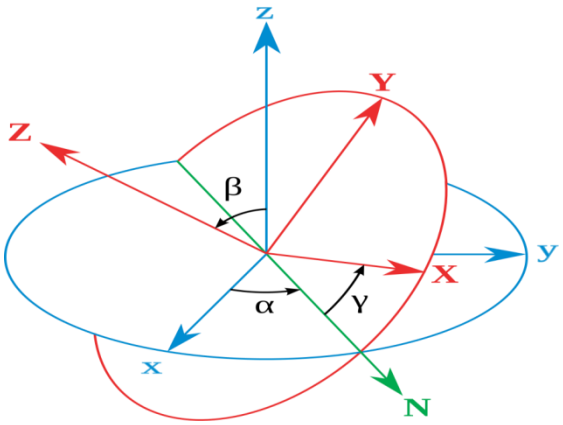


Fig.5: Euler angles

The advantages of Euler angle are the mathematics is easy and they are very easy to implement and to understand when compared with the quaternion .the storage Requirement is very less as they need only 3 components for the representation of any rotation.

Euler angle has several draw back the main problem facing is the gimbal lock. .gimbal is ring which rotate about an axis. Here the 2 axis may become in a straight line and they lose the degree of freedom. The main applications of Euler angle are used mainly in classical mechanics of rigid body and quantum mechanics of angular momentum.

4.2.2 Spatial Rotation Using Quaternion

In general Euler angle method is having a drawback called gimbal lock. Simply we can say it loss of degree of freedom. It happens when orientation of senor cannot be uniquely represented using Euler angle. The below figure illustrates the difference between the quaternion and Euler angle

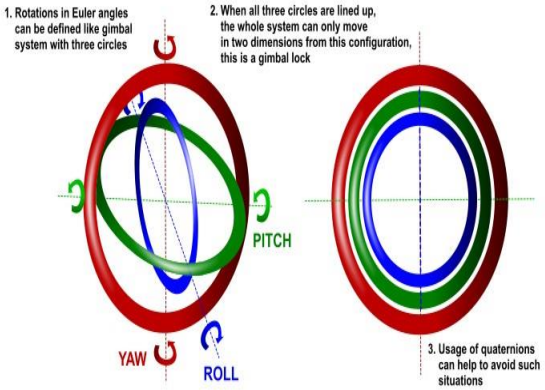


Fig.6: Comparison With and With Out Gimbal Lock

4.2.3 Quaternion

In general quaternion can be defined using symbols i, j, k .We call unit quaternion as versos. Here quaternion mathematically represents orientation and rotations of objects in 3D.

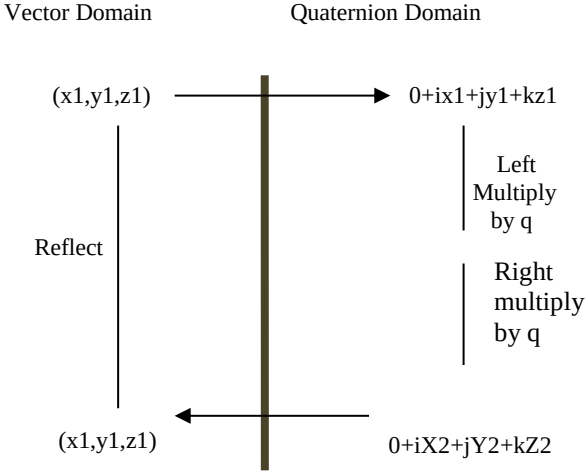


Fig.7: Vector Domain Versus Quaternion Domain.

When compared with Euler angles these are simple, numerically stable and efficient. Quaternion has important applications they are useful in various fields like they are used in mobile dynamics and flight dynamics and used in crystallographic texture. Quaternion has independent coordinate system and having easy composition.

5. Results

The measurement data is GPS and INS integrated system data with the state estimation using kalman filter. The algorithm which we have implemented is having mainly one routine which is implemented based on quaternion using GPS and Inertial measurement unit. Here we get GPS data using U-blox receiver and it having a clock speed of 32 kHz using RTC crystal. The IMU used for data collection is having 9DOF with 3 axes measurement and the outputs of it are processed by ATmega328 which is embedded on sensor board. Here we have used discrete time extended 4-state kalman filter to estimate the orientation of un-manned aerial vehicles.

In general, using the quaternion states in an EKF can be mathematically difficult. Here, we tried to make the quaternion math simple by converting the quaternion states into a Direction-Cosine-Matrix for use in the state dynamics and other measurement models. A quaternion purist will disagree with the implementation, but we feel it maintains the advantages of quaternions.

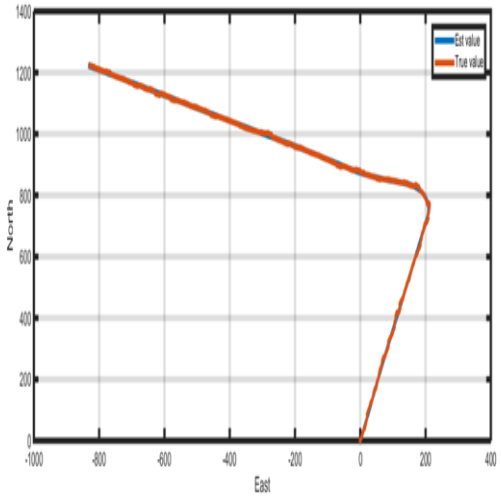


Fig.8: L-shape generated by EKF-based INS using quaternions and a 2D magnetometer.

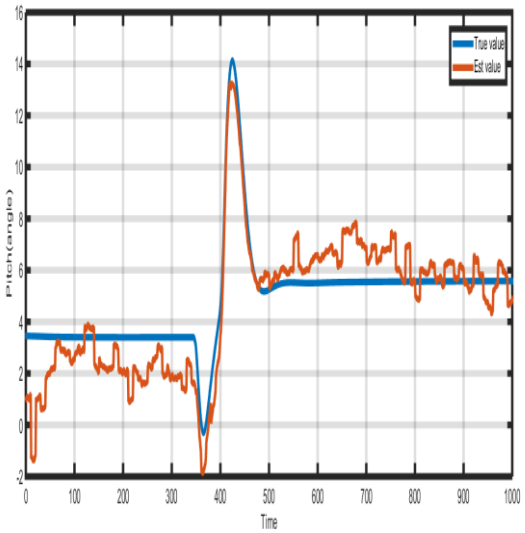


Fig.9: Pitch estimation of UAV by EKF-based INS using quaternions

The graphs which are obtained are having the minimum deviations in the calculation of various parameters of aerial vehicles using the integration of both GPS and Inertial navigation systems.

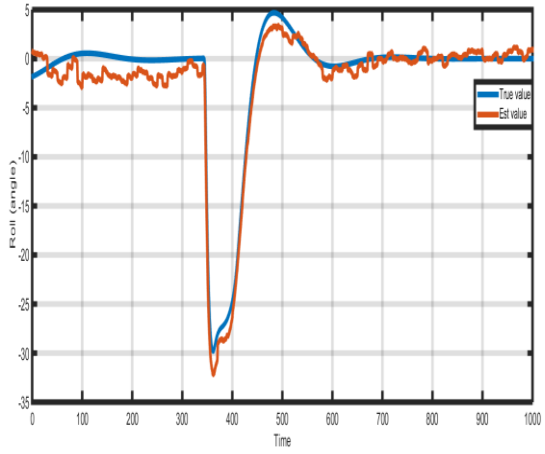


Fig.10: Roll estimation of UAV by EKF-based INS using quaternions

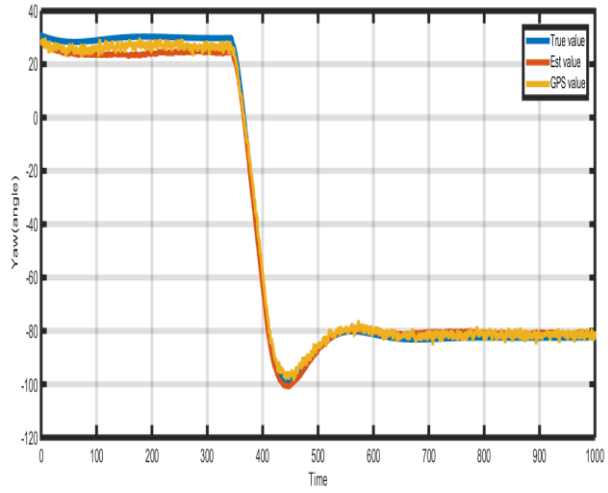


Fig.11: Yaw estimation of UAV by EKF-based INS using quaternions and a 2D magnetometer

Moreover we can reduce the error rate in the navigation systems by adding the adaptively in the kalman filter algorithm.

6. Conclusion

The results of the integrated navigation system are quite encouraging and the discrete time extended kalman filter method can be further improved with the addition of state dynamics, measurement models, modelling of error and estimation for gyro biases, etc.

7. References

[1] R Revathi, S Lakshminarayana, S Koteswara Rao, K S Ramesh, K.Uday Kiran, "Application of Maximum Entropy Method for Earthquake Signatures using GPSTEC", Proc. of SPIE, Vol. 9880, 988028,© 2016 SPIE • CCC code: 0277-786X/16/$18 • doi: 10.1117/12.2227500.

[2] R Revathi, S Lakshminarayana, S Koteswara Rao, K S Ramesh, K.Uday Kiran, "Observation of Ionospheric Disturbances for Earthquakes (M>4) Occurred During June 2013 to July 2014 in Indonesia using Wavelets, Proc. of SPIE.

[3] R Revathi, S Lakshminarayana, S Koteswara Rao, K S Ramesh, K.Uday Kiran, "Analysis of Seismo-Ionospheric Perturbations using Modified Covariance Algorithm" Proc. of SPIE Vol. 9877, 987730 • © 2016 SPIE,CCC code: 0277-786X/16/$18 • doi: 10.1117/12.2225887.

[4] Uma,G.aBrahmanandam,P.S.a,Kakinami,Y.b,Dmitriev, A.b,Latha Devi, N.S.M.P.a,Uday Kiran, K.a,Prasad, D.S.V.V.D.c,Rama Rao, P.V.S.c, Niranjan, K.c,Seshu Babu, C.d,Chu, Y.H.b, "Ionospheric responses to two large geomagnetic storms over Japanese and Indian longitude sectors", Journal of Atmospheric and Solar-Terrestrial PhysicsVolume 74, January 2012, Pages 94-110.

[5] Jhansi Rani, Sri Kavya, K.C. Kotamraju, S.K., Sree Teja, G., Snigdha, K., "Real time signal analysis for modeling the performance of UHF/VHF transceivers", International Journal of Applied Engineering Research,Volume 9, Issue 20, 2014, Pages 8063-8088.

[6] Khan, H., Madhav, B.T.P., Mallikarjun, K., Bhaskar, K., Sri Harsha, N., Nakka, M., "Uniplanar wideband/narrow band antenna for wlan application", World Applied Sciences Journal Volume 32, Issue 8, 2014, Pages 1703-1709.

[7] Venkata Narayana, M.Email Author, Imamdi, G., Khan, H., Lakshmi Durga, P.V.N., Sirisha, N., Praveen Kumar Reddy, R., Chandan Krishna, Y. View Correspondence (jump link), "Design of electrically small top loaded antennas for GPS applications", ARPN Journal of Engineering and Applied Sciences,Volume 10, Issue 22, 2015, Pages 10281-10287.

[8] Raman, Y.S.V., Madhav, B.T.P., Mounika, G., Sai Teja, K., Sai Kumar, S.B.V.N. And Sri Harsha, K., 2016. Analysis Of Circularly Polarized Notch Band Antenna With Dgs. Arpn Journal Of Engineering And Applied Sciences, 11(17), Pp. 10140-10150.

[9] Madhav, B.T.P., Mohan Reddy, S.S., Sharma, N., Ravindranath Chowdary, J., Pavithra, B.R., Kishore, K.N.V.S., Sriram, G. And Sachin Kumar, B., 2013. Performance Characterization Of Radial Stub Microstrip Bow-Tie Antenna. International Journal Of Engineering And Technology, 5(2), Pp. 760-764.

[10] Ajay Babu, M., Madhav, B.T.P., Naga Vaishnavi, D., Radhakrishna, P., Bharath, N., Madhuri, K., Bhavani Prasad, K. And Harish, K., 2015. Flared V-Shape Slotted Monopole Multiband Antenna With Metamaterial Loading. International Journal On Communications Antenna And Propagation, 5(2), Pp. 93-97.

[11] Aditya Varma, K.V., Manideep, T. And Asadi, S.S., 2016. A Critical Comparison Of Quantity Estimation For Gated Community Construction Project Using Traditional Method Vs Plan Swift Software: A Case Study. International Journal Of Civil Engineering And Technology, 7(6), Pp. 707-713.

[12] Murali, A., Kakarla, H.K. And Venkat Reddy, D., 2016. Integrating Fpgas With Trigger Circuitry Core System Insertions For Observability In Debugging Process. Journal Of Engineering And Applied Sciences, 11(12), Pp. 2643-2650.

[13] Mohan Reddy, S.S., Mallikarjuna Rao, P. And Madhav, B.T.P., 2015. Asymmetric Defected Ground Structured Monopole Antenna For Wideband Communication Systems. International Journal On Communications Antenna And Propagation, 5(5), Pp. 256-262.